nature climate change

Article

https://doi.org/10.1038/s41558-022-01509-z

Snowmelt risk telecouplings for irrigated agriculture

Received: 20 October 2021

Accepted: 22 September 2022

Published online: 31 October 2022

Check for updates

Yue Qin[1] ✉, Chaopeng Hong[2], Hongyan Zhao[3], Stefan Siebert[4,5], John T. Abatzoglou[6], Laurie S. Huning[7,8], Lindsey L. Sloat[9], Sohyun Park[10,11], Shiyu Li[1], Darla K. Munroe[12], Tong Zhu[1], Steven J. Davis[8,13] and Nathaniel D. Mueller[14,15] ✉

Climate change is altering the timing and magnitude of snowmelt, which may either directly or indirectly via global trade affect agriculture and livelihoods dependent on snowmelt. Here, we integrate subannual irrigation and snowmelt dynamics and a model of international trade to assess the global redistribution of snowmelt dependencies and risks under climate change. We estimate that 16% of snowmelt used for irrigation is for agricultural products traded globally, of which over 70% is from five countries. Globally, we observe a prodigious snowmelt dependence and risk diffusion, with particularly evident importing of products at risk in western Europe. In Germany and the UK, local fraction of surface-water-irrigated agriculture supply exposed to snowmelt risks could increase from negligible to 16% and 10%, respectively, under a 2 °C warming. Our results reveal the trade-exposure of agricultural supplies, highlighting regions and crops whose consumption may be vulnerable to changing snowmelt even if their domestic production is not.

Snowpack acts as an important natural reservoir that can provide seasonal water resources during crop growing seasons[1,2]. Climate change, however, has already begun to alter global patterns of snowfall, causing earlier melting and contributing to decreasing magnitude of snowmelt runoff in the long run[3–6]. Although such changes in snowmelt-derived water resources are often cited as a key threat to irrigated agriculture and global food security[7–11], only a few recent studies have effectively analysed such risks by reconciling snowpack and irrigation water demand dynamics[12–16]. Even fewer efforts have been taken to characterize such risks at the global scale with subannual temporal resolutions[14–16].

Changing snowmelt will not only pose threats to local irrigated agricultural production that historically depends on such seasonal water resources[13,16] but may also threaten global food security through international trade. Earlier studies have extensively evaluated global virtual water transfer embodied in agricultural trade[17–28], with a primary focus on annual total blue water and green water savings and/or losses[18–21]. A few recent studies started exploring the linkages between agricultural trade and other important water-related risks, such as regional water scarcity[24,25], grey water-associated pollution[17,26,27], groundwater depletion[22] and unsustainable virtual water flows[28]. However, it remains unclear how international trade could reshape

[1]College of Environmental Science and Engineering, Peking University, Beijing, China. [2]Institute of Environment and Ecology, Shenzhen International Graduate School, Tsinghua University, Shenzhen, China. [3]School of Environment, Beijing Normal University, Beijing, China. [4]Department of Crop Sciences, University of Göttingen, Göttingen, Germany. [5]Centre of Biodiversity and Sustainable Land Use (CBL), University of Göttingen, Göttingen, Germany. [6]Management of Complex Systems Department, University of California, Merced, CA, USA. [7]Department of Civil Engineering and Construction Engineering Management, California State University, Long Beach, CA, USA. [8]Department of Civil and Environmental Engineering, University of California, Irvine, CA, USA. [9]World Resources Institute, Washington, DC, USA. [10]Computational and Data Sciences, George Mason University, Incheon, South Korea. [11]Department of Geography, The Ohio State University, Columbus, OH, USA. [12]Lincoln Institute of Land Policy, Cambridge, MA, USA. [13]Department of Earth System Science, University of California, Irvine, CA, USA. [14]Department of Ecosystem Science and Sustainability, Colorado State University, Fort Collins, CO, USA. [15]Department of Soil and Crop Sciences, Colorado State University, Fort Collins, CO, USA. ✉e-mail: qinyue@pku.edu.cn; nathan.mueller@rams.colostate.edu

https://doi.org/10.1038/s41558-022-01509-z

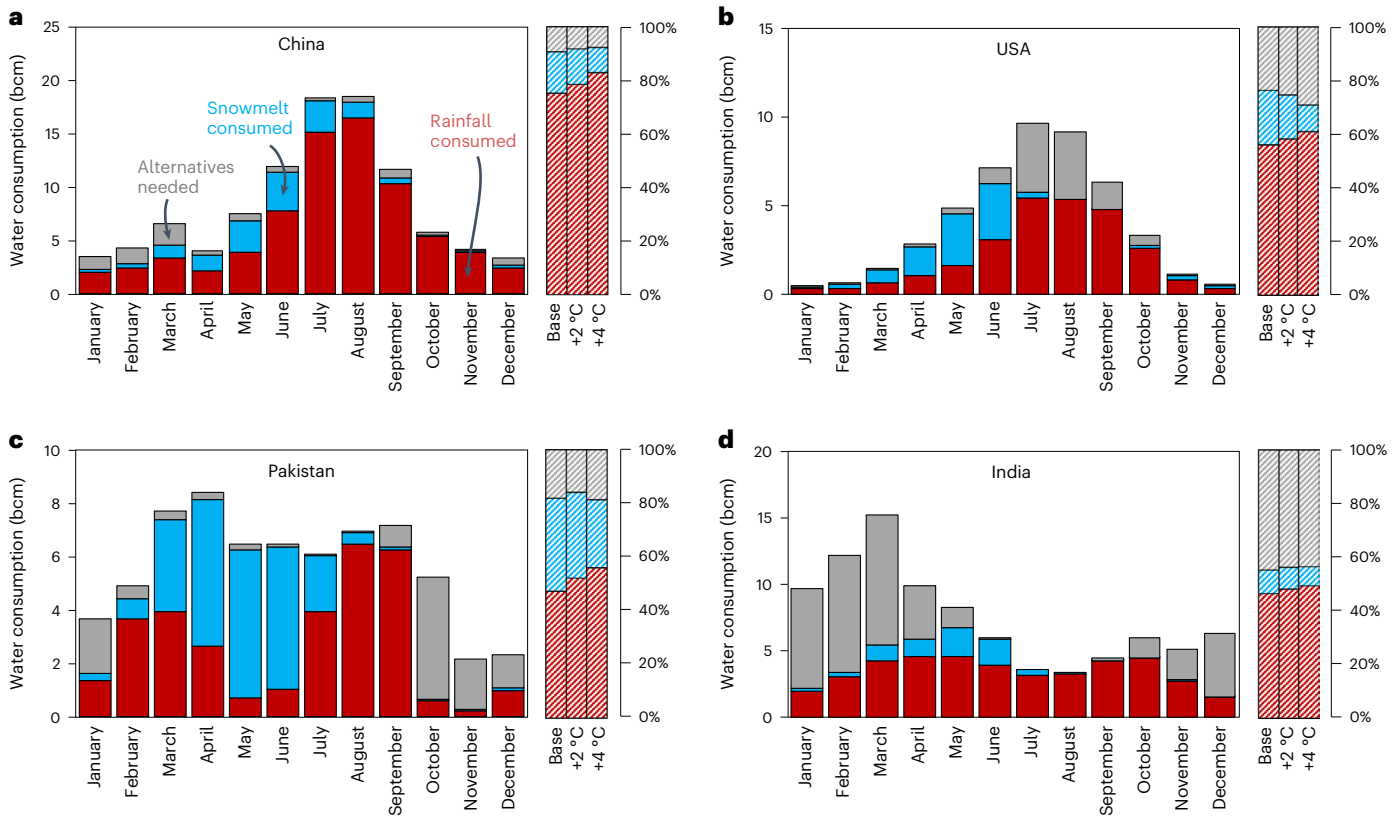

Fig. 1 | GTAP region-level surface irrigation water demand met by different water sources (1985–2015). a–d, Monthly runoff from snowmelt runoff, rainfall runoff and alternative water demand for China (**a**), the USA (**b**), Pakistan (**c**) and India (**d**) are shown in stacked bars inside the box, where the shaded red, blue and grey bars denote the corresponding contributions from rainfall runoff, snowmelt runoff and alternative surface-water sources (for example, reservoir storage and interbasin transfer), respectively. Annual average percentage contributions from each source are shown in striped bars outside the box for the baseline climate (base: 1985–2015), +2 °C and +4 °C warming scenarios, respectively.

the exposure of food supplies across the world to changing snowmelt under a warming climate.

Here, we build an integrated framework to quantify the interactions among subannual irrigation water demand, snowmelt runoff dynamics and international trade of agricultural products. Details of our analytical approach are provided in the Methods. In summary, we characterize the spatial pattern of irrigation snowmelt runoff transfer embodied in international trade throughout the whole global supply chain and the resulting telecouplings[29] of agricultural snowmelt risks due to climate change by integrating irrigation surface-water consumption estimates primarily based on the global crop water model (GCWM)[30–32], snowmelt and rainfall runoff simulations from the TerraClimate database[33] and a multiregional input–output (MRIO) model of international trade. Using the global MRIO model of trade supported by the global trade analysis project (GTAP)[34,35], we thus track the irrigation snowmelt runoff, rainfall runoff and alternative water flow embodied in global trade, as well as the virtual flow of crop-specific production exposed to snowmelt risks to illustrate how global trade reshapes snowmelt dependence and risks for irrigated agriculture (Methods). Our study focuses on surface water and associated irrigated agriculture unless otherwise stated.

Source attribution of irrigation surface-water consumption

Aggregating water source attributions in each basin, we illustrate the monthly breakdown of water sources that meet surface-water demand in selected countries which experience substantial irrigation snowmelt flow embodied in trade (Fig. 1 and Extended Data Figs. 1 and 2). Taking the USA as an example, snowmelt runoff contribution to total water demand is generally largest in spring and decreases evidently by midsummer. As a result, both rainfall runoff and alternative water consumption increase in summer when monthly water demand is the largest, while alternative water quickly decreases to a negligible level afterwards along with declining irrigation water demand. Despite notable differences in the magnitude and seasonality of irrigation water demand across selected countries, in almost all cases, countries display a dominating annual average contribution from rainfall runoff under the baseline climate. In addition, all four countries demonstrate a shrinking annual average contribution from snowmelt runoff under 2 °C and 4 °C warming scenarios, indicating decreasing snowmelt runoff availability in crop growing seasons due to climate change. Nevertheless, such decreases may not always lead to increasing demand for alternative water supply, as decreases may be partly or fully compensated by increasing rainfall runoff.

Global irrigation flow by water sources

Figure 2 presents agricultural irrigation surface-water consumption embodied in trade along the whole global supply chain broken down by water sources, with net importers in red and exporters in blue. As shown in the snowmelt transfer map (Fig. 2a), net snowmelt exporters mainly include South Asia (Pakistan and India), East Asia (China), Argentina and the USA, locations that often use a substantial amount of snowmelt runoff for irrigated agriculture production. In comparison, net snowmelt importers are mainly distributed in Western Europe (Germany, the UK and France), the Middle East, Brazil, Canada, Africa and Australia. These countries usually either locally consume marginal snowmelt for irrigation

https://doi.org/10.1038/s41558-022-01509-z

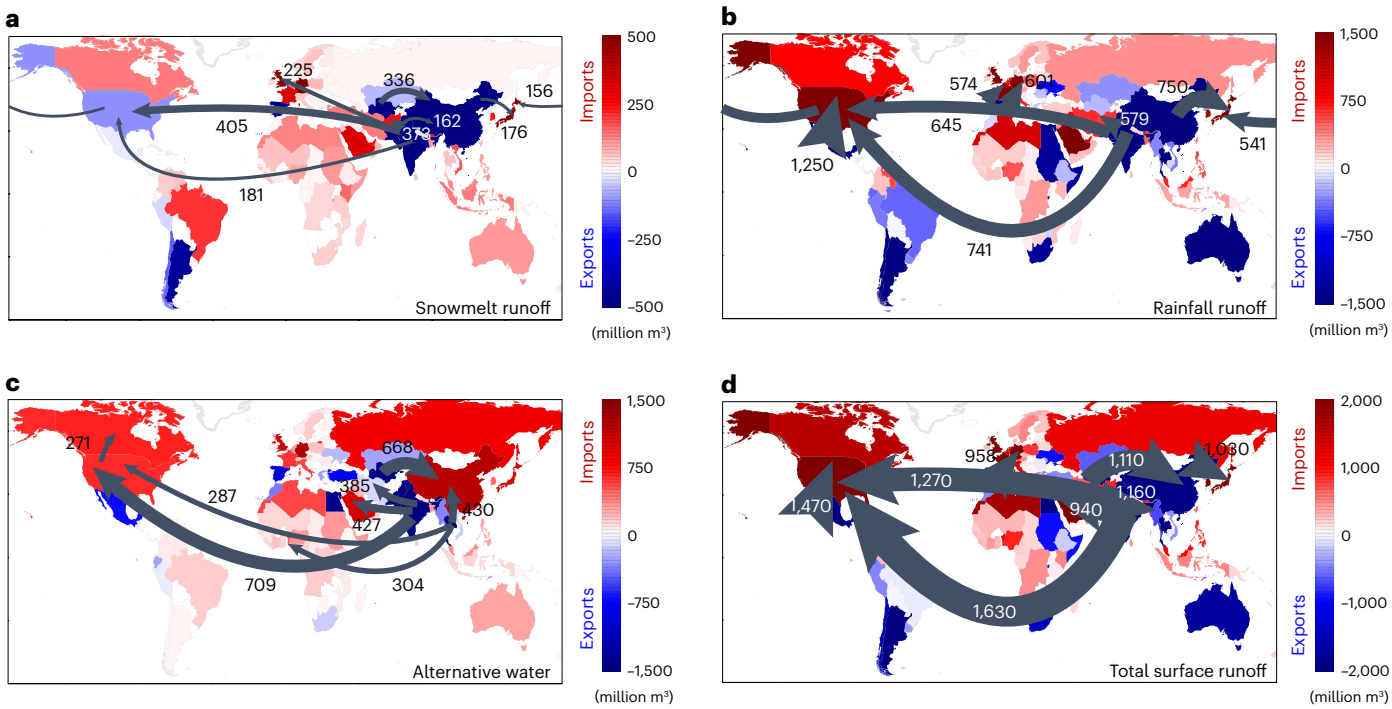

Fig. 2 | Source-specific irrigation surface-water transfer embodied in international trade. a–**d**, GTAP region-level virtual transfer of snowmelt runoff (**a**), rainfall runoff (**b**) and alternative water (**c**), as well as their sum (**d**), embodied in international trade throughout the whole global supply chains for surface-water-irrigated agriculture. In each panel, arrows depict the top eight largest interregional fluxes of respective water transfer. Global trade reshapes water source dependence via simultaneously redistributing all three water sources. GTAP region base map is modified from ESRI World Countries[51].

purposes (African countries) or they may depend on snowmelt for local production but have both relatively high imports and exports of snowmelt runoff (for example, Canada). Globally, the top five agricultural snowmelt exporters (Pakistan, 26%; China, 14%; the USA, 13%; India,10%; and the Rest of Former Soviet Union (RFSU) 8%) together account for 71% of irrigation snowmelt exports, as well as 76% of production-based snowmelt consumption. In comparison, the top five snowmelt importers (the USA, China, Germany, the UK and Japan) only make up 32% of global total imports, with the remaining imports widely distributed across the rest of the world. Although snowmelt runoff consumption for irrigated agriculture production is primarily concentrated in a few regions, almost the entire rest-of-the-world indirectly consumes snowmelt via international trade (Supplementary Fig. 1).

Rainfall runoff (Fig. 2b and Supplementary Fig. 2) and alternative water flow (Fig. 2c and Supplementary Fig. 3) demonstrate notably different spatial patterns and considerably larger magnitudes than snowmelt runoff. For instance, Asian countries, Australia and South America are primary net rainfall exporters, whereas net importers are concentrated in North America, Middle East, Africa and Europe. Net alternative water importers are predominantly located in China, Russia, North America, western Europe, Africa and Australia, with Southeast Asia and Central Asia being major net exporters. Global total surface irrigation flow (Fig. 2d) represents net combinations of snowmelt, rainfall and alternative water transfer and mostly resembles the spatial pattern of its largest component—rainfall runoff.

The largest interregional fluxes of varying water sources highlight a similar dominating feature along the global supply chain—the exports of surface-water embodied in trade from Asian countries (India, Pakistan and China) to US consumers (Fig. 2). For instance, Pakistan alone exports 405, 645 and 223 million m^3 of irrigation snowmelt, rainfall and alternative water to the USA via trade. Global maximum interregional flows of rainfall runoff and alternative water are roughly 3.1 and 1.7 times that of snowmelt runoff. Despite the dominating US imports of different sources of interregional surface fluxes, the USA also exports considerable surface runoff and alternative water via diverse channels at individually smaller magnitudes, yet the overall total exports can be large (Supplementary Figs. 4–6). Therefore, some of the leading snowmelt importers are simultaneously leading exporters (the USA and China; Supplementary Fig. 4).

Supplementary Figs. 7 and 8 depict the balance of surface irrigation water for the top five net importers and exporters, along with details of water sources and crop species accounting for traded surface irrigation water. Globally, about 12, 66 and 30 billion cubic metres (bcm) of irrigation snowmelt, rainfall and alternative water are embodied in trade, making up, respectively, 16%, 20% and 18% of global surface irrigation water consumption from each water source. Regarding snowmelt runoff embodied in trade, paddy rice (25%) and wheat (24%) together contribute half of global flow, followed by vegetables, fruits and nuts (19%), oil seeds (17%), and other cereal grains (10%).

Pakistan is by far the largest net snowmelt exporter (-3.2 bcm), followed by India, RFSU, China and Spain; the primary net snowmelt importers are Germany, the UK and Japan. The prodigious imbalance in the snowmelt flow of Pakistan and India is due to exports of paddy rice (1.7 and 0.3 bcm) and wheat (0.7 and 0.66 bcm). Comparatively modest snowmelt imports in Pakistan and India are dominated by vegetables and fruits (0.02 and 0.08 bcm). Paddy rice (0.6 bcm) and other cereal grains (0.4 bcm), along with wheat (0.39 bcm), make up the largest snowmelt exported from China, whereas imported oil seeds and paddy rice offset 0.5 and 0.13 bcm, respectively.

Germany is the largest net snowmelt importer, whose snowmelt imports (0.56 bcm) exceed that of any country other than the USA (1.46 bcm) and China (0.9 bcm), yet the last two are also among the top three snowmelt exporters (1.58 and 1.76 bcm exports in the USA and China, respectively), hence largely offset their snowmelt imports.

https://doi.org/10.1038/s41558-022-01509-z

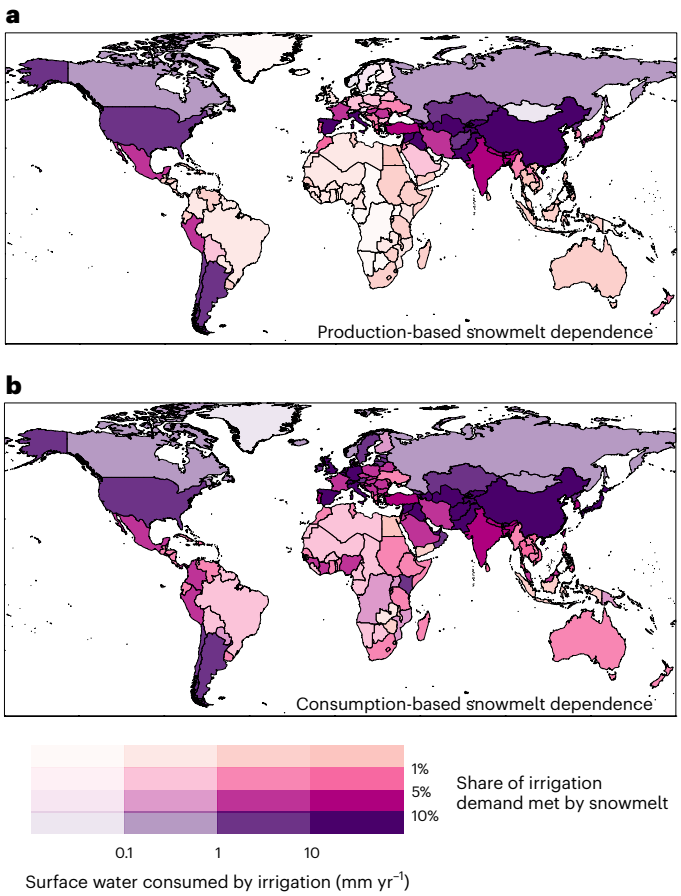

Fig. 3 | Global production-based and consumption-based hotspots of snowmelt-dependence for irrigated agriculture. a,**b**, Maps showing production-based snowmelt dependence (**a**) and consumption-based snowmelt dependence (**b**). Colours indicate GTAP region-level average share of irrigation surface-water demand met by snowmelt runoff and the intensity of shading indicates the average irrigation surface-water demand normalized by GTAP region area. Global trade slightly reduces the snowmelt-dependence of consumption in a few countries/regions by dispersing the dependence worldwide. GTAP region base map is modified from ESRI World Countries[51].

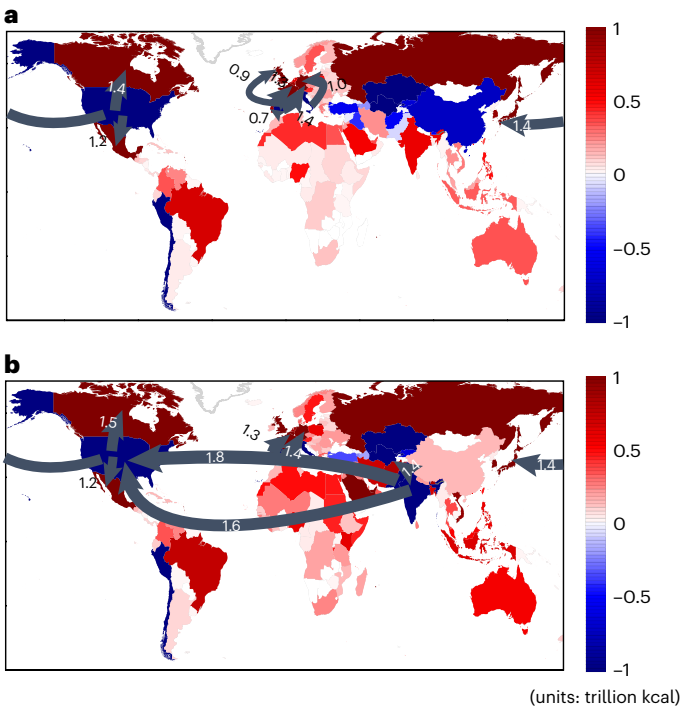

Fig. 4 | Virtual transfer of agricultural products at risk embodied in international trade. a,**b**, Virtual transfer of production at risk throughout the whole global supply chains under 2 °C (**a**) and 4 °C (**b**) warming scenarios. Arrows depict the top eight largest interregional fluxes of surface-water-irrigated agricultural products exposed to snowmelt risks due to international trade. GTAP region base map is modified from ESRI World Countries[51].

The balance of snowmelt trade is similar in Germany, the UK, Japan and Saudi Arabia, with substantial snowmelt imports embodied in paddy rice, wheat and vegetables, fruits and nuts. Notably, top net snowmelt exporters/importers (Pakistan/Germany) are often simultaneously among the largest rainfall and alternative water exporters/importers, yet China and many less predominant snowmelt traders (Australia) can either be net exporters or importers depending on water sources examined (Fig. 2 and Supplementary Figs. 4–7).

International trade reshapes water source dependence

International trade simultaneously redistributes snowmelt, rainfall and alternative water, which consequently reshapes local water source dependence for irrigated agriculture. Integrating the share of irrigation water demand met by snowmelt runoff, GTAP-level average irrigation surface-water demand, together with snowmelt transfer embodied in trade, Fig. 3 illustrates snowmelt-dependence maps for irrigated agriculture under both production-based and consumption-based accounting (Methods). Countries or regions that require substantial surface water for irrigation (intensity of shading) and largely rely on snowmelt runoff (colours) are particularly snowmelt-dependent. As revealed by Fig. 3, global trade results in prodigious diffusion of snowmelt-dependence worldwide on consumption-based perspective compared to production-based perspective.

Under production-based accounting, roughly 60% of the population (4.3 billion) and gross domestic product (GDP) based on purchasing power parity (PPP, ~70 trillion current international $) are located in 20% of global GTAP regions that are identified to be relatively snowmelt-dependent (defined as obtaining >5% of annual total irrigation surface water from snowmelt runoff and consuming >1 mm yr^{-1} total irrigation surface water; Methods). In comparison, our consumption-based accounting finds the number of GTAP regions with relatively high snowmelt-dependence more than doubled due to their imports (from 20% to 53%) and the associated snowmelt-dependent population and GDP increased by ~20% (0.8 billion) and ~30% (PPP, ~20 trillion current international $), thus reaching 71% and 75% of the global total, respectively.

In particular, snowmelt-dependence across Africa, northern parts of South America and Australia is notably higher when accounting for snowmelt imports embodied in trade. In comparison, irrigated consumption in Asia (for example, China and India), North America and southern parts of South America (for example, Argentina) can become less dependent on snowmelt when accounting for trade—primarily due to a disproportionately large share of snowmelt runoff exports embodied in trade compared with their respective production-based water source dependence (Fig. 3 and Supplementary Fig. 9). Nevertheless, these regions generally still have the highest snowmelt-dependence across the globe under consumption-based accounting.

Virtual transfer of irrigated production at risk

Following an earlier definition of basins at risk of snowmelt changes[16], we estimate crop-specific irrigated production that is exposed to

https://doi.org/10.1038/s41558-022-01509-z

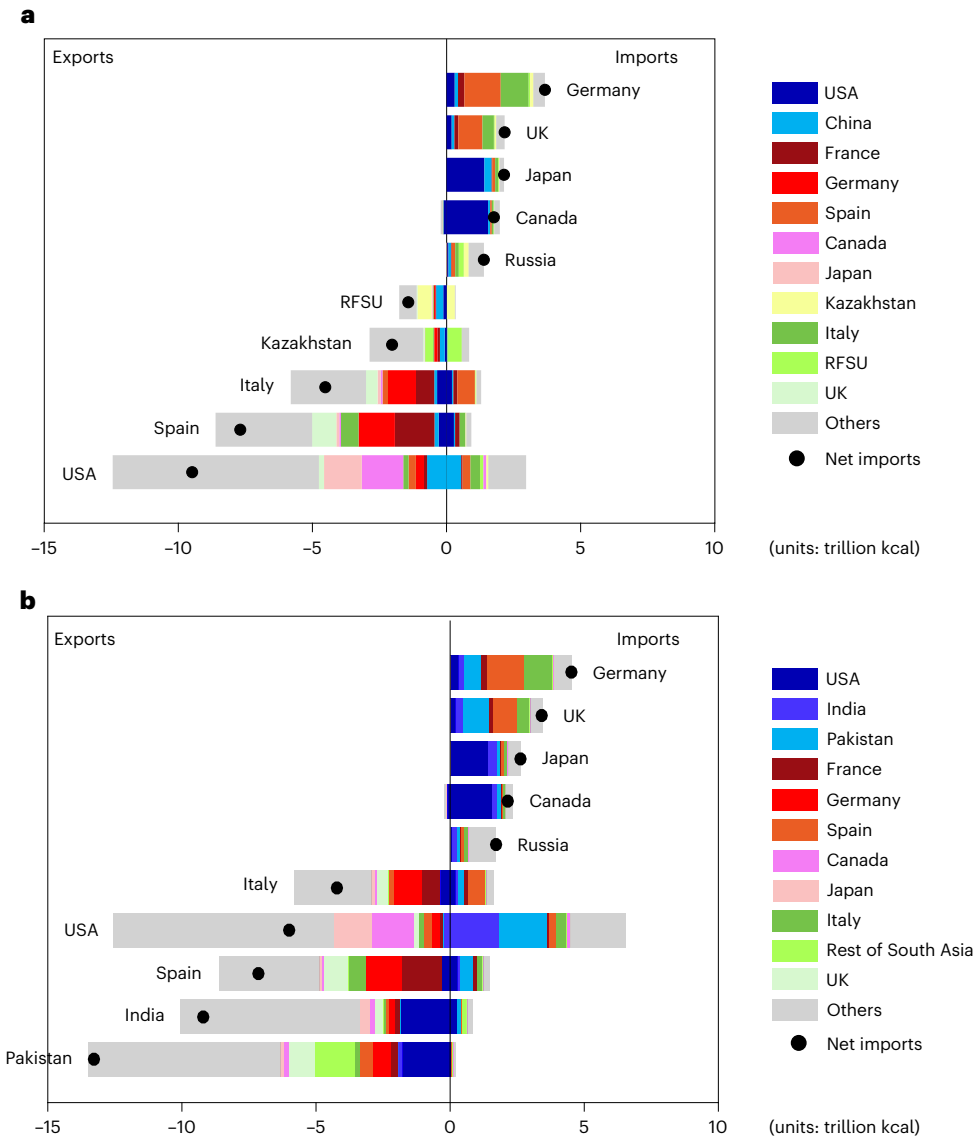

Fig. 5 | Virtual transfer of agricultural production at risk detailed across trading partners. a,**b**, Virtual flow of surface-water-irrigated agricultural products exposed to snowmelt risks throughout the whole global supply chains under 2 °C (**a**) and 4 °C (**b**) warming scenarios broken down by major trading partners. Black dots represent net virtual transfer of surface-water-irrigated agricultural products at risk.

snowmelt risks (defined for historically snowmelt-dependent agriculture, which will experience decreasing snowmelt availability in crop growing seasons and simultaneously increasing demand for alternative water supplies due to climate change; Supplementary Fig. 10). Aggregating grid-level production at risk belonging to each GTAP region, we obtain GTAP-level crop-specific production at risk (Methods). We further use our GTAP trade data to track the virtual transfer of such crop-specific risks throughout the whole global supply chains (Extended Data Figs. 3 and 4) under both warming scenarios.

Similar to the snowmelt runoff flow embodied in trade, irrigated agriculture production exposed to snowmelt risks demonstrates an obvious diffusion from a few countries mostly concentrated in Asia, North America, Chile and Western Europe to the rest of the world. Arrows in Fig. 4 represent the largest interregional flow of production at risk. The dominant global features under both 2 °C and 4 °C warming scenarios are exports from the USA to Canada (~1.5 trillion kcal), Japan (~1.4 trillion kcal) and Mexico (~1.2 trillion kcal), and exports from Spain to Germany (~1.4 trillion kcal), France (~1.3 trillion kcal) and the UK (~0.9 trillion kcal). The 4 °C warming scenario also demonstrates notable exports from South Asia (Pakistan) to the USA (~1.8 trillion kcal) and the UK (~1 trillion kcal) due to increased production at risk in South Asia under a warmer climate (Supplementary Figs. 10 and Extended Data Figs. 3 and 4).

Figure 5 presents the balance of irrigated agriculture production exposed to snowmelt risks for the top five net importers/exporters under both 2 °C and 4 °C warming scenarios, along with details of countries/regions accounting for traded production at risk. Primary net exporters (Spain, the USA, Italy, Pakistan and India) and importers (Germany, the UK and Japan) are similar to those for snowmelt runoff, particularly for a 4 °C warming (Supplementary Fig. 4). Germany and the UK display a similar regional attribution of production at risk, with substantial imports from Spain and Italy, as well as from Pakistan and the USA under the 4 °C warming. Likewise, Japan and Canada import considerable production at risk primarily from the USA. Exports of production at risk for net exporters are much more spatially dispersed (Fig. 5 and Supplementary Figs. 11 and 12). For instance, Italy and Spain mainly outsource their production at risk towards Germany, France, the UK, the USA, and many other countries under both warming scenarios,

https://doi.org/10.1038/s41558-022-01509-z

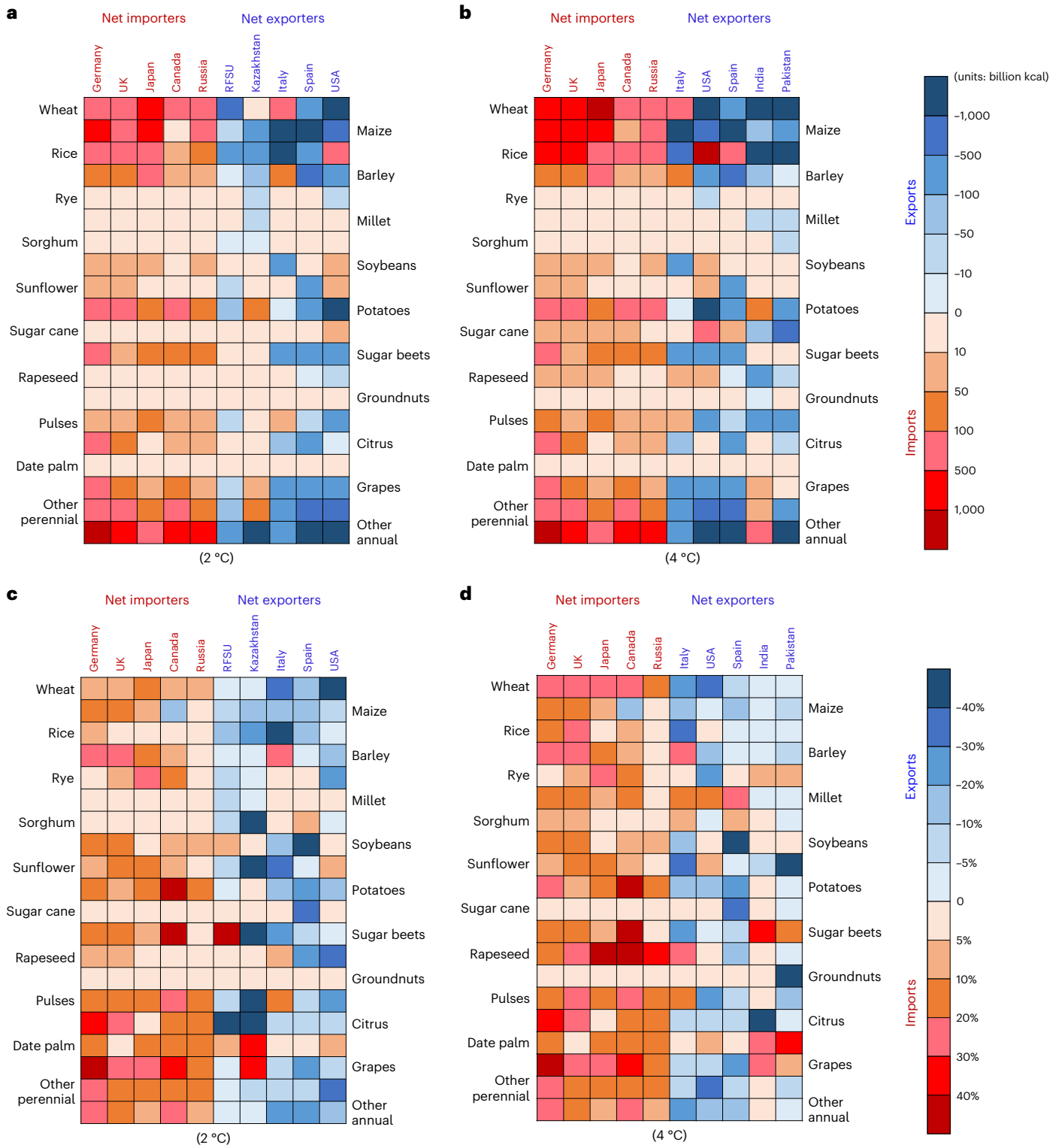

Fig. 6 | Crop-specific production at risk for top importers and exporters. **a**,**b**, Importing and exporting quantity of surface-water-irrigated production exposed to snowmelt risks throughout global supply chains for 2 °C (**a**) and 4 °C (**b**) warming scenarios. **c**,**d**, The fraction of local surface-water-irrigated agricultural products at risk for the top five net importers and exporters broken down by major crop species for 2 °C (**c**) and 4 °C (**d**) warming scenarios. Net importing and exporting regions are ordered by their respective total traded production at risk, with higher net imports to the left and higher net exports to the right in each panel.

whereas the USA mainly outsources their production at risk to Canada, Japan, China, Germany and others. Trading patterns for production at risk are more or less similar under the 2 °C and 4 °C warming scenarios, though their top net exporters are not identical due to different spatial distributions of basins at risk under the two warming scenarios and higher overall production at risk under the 4 °C warming scenario (Supplementary Fig. 10).

Figure 6a,b illustrate the crop-specific mix of irrigated agricultural production at risk embodied in trade for top five net importers and exporters. Despite noticeable regional variations, wheat, maize,

rice and other annuals are generally those most important products via which countries outsource/import production that are exposed to snowmelt risks.

International trade redistributes agricultural products exposed to snowmelt risks, placing countries or regions at risk that are otherwise not susceptible to changing snowmelt runoff for their own domestic production. As shown in Supplementary Fig. 13, there is a global dominating pattern of snowmelt risks diffusion, which is particularly prodigious across Western Europe, Canada, Russia, Africa and other countries. Focusing on top importers and exporters of products at risk (Fig. 6), we find that, under the 2 °C (4 °C) warming scenario, the fraction of surface-water-irrigated crops exposed to changing snowmelt could increase from 0% to 16% (19%) in Germany and to 10% (16%) in the UK, when factoring in trade. Notable variations across crop species exist. For instance, global trade increases the fraction of local surface-water-irrigated agricultural products exposed to snowmelt risks for grapes, wheat and rice by 43% (43%), 9% (23%) and 8% (16%) in Germany and 22% (22%), 7% (27%) and 5% (20%) in the UK under the 2 °C (4 °C) warming scenario (Fig. 6c,d). In comparison, the major snowmelt risks outsourcing occurs in the USA, Spain, Italy, Central Asia and other countries. For example, Italy, the USA and Spain could reduce their fraction of products at risk by 20% (19%), 18% (15%) and 14% (12%), respectively. Under consumption-based accounting, the share of irrigated rice and wheat exposed to snowmelt risks in Italy decrease by 41% (36%) and 33% (29%) due to a 2 °C (4 °C) warming, respectively. Therefore, snowmelt risks importing countries (for example, Germany and the UK) become more exposed to changing snowmelt under a warming climate due to substantial imports of production at risk, yet countries such as Italy, the USA and Spain can partly outsource their exposure to climate-induced snowmelt risks via trade, although this trade only affects local food supply available for consumption and does not enhance local farmers' economic resilience to potential snowmelt risks.

Discussion

Despite increasing recognition of the agricultural risks associated with changing snowmelt, the telecouplings of such unique snowmelt risks due to international trade have remained unknown. Our study builds an integrated framework to couple historical subannual irrigation water demand, snowmelt runoff dynamics and an accounting of international trade to reveal the first-order global dimension of agricultural snowmelt dependence and risks from changing snowmelt under a warming climate.

We identify a global dominating pattern of snowmelt dependence and risk diffusion due to international trade, with notably more countries indirectly exposed to changing snowmelt under climate change due to their imports of agricultural goods. Like countries that are directly exposed to snowmelt risks, these importing countries may need to enhance local agricultural resilience either by improving local crop yields, switching and diversifying trading partners and/or taking demand-side adaptation practices (for example, food loss and waste mitigation). International trade does help mitigate the fraction of irrigated products at risk in a few risks-outsourcing countries such as Italy, the USA and Spain, yet the situation is more dire for some of the topmost net exporters of agricultural products at risk, especially under the 4 °C warming scenario (Pakistan and India)[13]. Although exported at risk crops are not used for local food supply, their production remains financially critical for local farmers' livelihoods. As a result, countries directly facing snowmelt risks are still in critical need of adaptation through improving local irrigation efficiency[36–38], investing in sustainable alternative water supplies[39,40] and/or switching crop species[41]. Therefore, worldwide snowmelt risk diffusion will spread the climate adaptation needs and is also likely to be conducive to forming wider consensus on climate change mitigation, which will play a fundamental role in resolving snowmelt risks induced by a warming climate.

Limitations and caveats apply to our study. First, we use a high spatial–temporal resolution TerraClimate database with a water balance model to capture the first-order snowmelt runoff dynamics. Despite the simplicity, our simulated subannual runoff and snow fraction to total water supply generally demonstrate reasonable performance across the globe (Supplementary Notes). Second, our model does not explicitly simulate glacier dynamics, which would bring increasing runoff in the near future (for example, in high mountain Asia)[12,13,42], yet considerable discharge reductions in a longer period[43–46]. We thus could not capture the short- to medium-term buffer effect in water supply from receding glaciers, whereas our estimates of snowmelt risks are likely to be conservative in the long run. Third, due to data availability, we fix global irrigation land area as that in MIRCA2000 in GCWM interannual historical blue water simulation, yet adjustments are made on the basis of FAO area equipped with irrigation data (Methods). Irrigation (as well as planting and harvest seasons) and other water demands are held fixed under a warming climate due to competing mechanisms and substantial uncertainties around future irrigation water consumption (for example, increasing evapotranspiration and improved water use efficiency with increasing CO_2; ref. [47]) and the inability to predict future land use changes and farmers' adaptation strategies[48]. Sensitivity studies are therefore conducted to evaluate the implications of changing water consumption under warming scenarios (Supplementary Notes and Supplementary Fig. 14). Fourth, estimation of source-specific virtual water flows (for example, snowmelt runoff) can vary on the basis of methodology, yet the two dominant GTAP and FAO-based trading models demonstrate a predominant snowmelt dependence and risk diffusion across the globe (Supplementary Figs. 15–18), as well as evident risks importing across western European countries and, to a less extent, in Canada, Africa, Russia and Australia (Supplementary Figs. 13 and 18). Finally, we use the latest 2014 GTAP trade matrix under warming scenarios, which can be a potential limitation of our study. While predicting how global trading patterns would change is beyond the scope of our study, sensitivity analyses show a similar share of population and GDP located in snowmelt-dependent regions when accounting for socioeconomic changes (Supplementary Fig. 19 and Supplementary Notes).

Despite the progress human society has made on improving food security over the past two decades, we are not on-track to achieve either zero hunger by 2030 or meet global nutrition targets[49,50]. Entering this new decade, improving food system resilience is becoming increasingly challenging yet crucial, with daunting challenges such as a changing climate redistributing seasonal water sources (snowmelt runoff), growing population and unpredictable global crises (COVID-19). Global trade transmits climate risks to regions where they did not otherwise exist and tends to distribute those risks across more regions. Characterizing the global telecouplings of climate risks to irrigated agriculture is important for understanding how trade both transmits and pools such risks. Our findings thus highlight the global implications of the unique dynamic risks related to changes in snowmelt, revealing the broader stakes of climate adaptation strategies.

Online content

Any methods, additional references, Nature Research reporting summaries, source data, extended data, supplementary information, acknowledgements, peer review information; details of author contributions and competing interests; and statements of data and code availability are available at https://doi.org/10.1038/s41558-022-01509-z.

References

1. Waliser, D. et al. Simulating cold season snowpack: impacts of snow albedo and multi-layer snow physics. *Clim. Change* **116**, 425–425 (2013).
2. Li, D. Y., Wrzesien, M. L., Durand, M., Adam, J. & Lettenmaier, D. P. How much runoff originates as snow in the western United States,

and how will that change in the future? *Geophys. Res. Lett.* **44**, 6163–6172 (2017).
3. Huning, L. S. & AghaKouchak, A. Mountain snowpack response to different levels of warming. *Proc. Natl Acad. Sci. USA* **115**, 10932–10937 (2018).
4. Stewart, I. T., Cayan, D. R. & Dettinger, M. D. Changes in snowmelt runoff timing in western North America under a 'business as usual' climate change scenario. *Clim. Change* **62**, 217–232 (2004).
5. Chaulagain, N. P. https://doi.org/10.1007/978-3-319-13743-8_15. in *Dynamics of Climate Change and Water Resources of Northwestern Himalaya* (eds Joshi, R. et al.) 191–199 (Springer, 2015).
6. Stewart, I. T., Cayan, D. R. & Dettinger, M. D. Changes toward earlier streamflow timing across western North America. *J. Clim.* **18**, 1136–1155 (2005).
7. Easterling, W. E. et al. in *Climate Change 2007: Impacts, Adaptation and Vulnerability* (eds Parry, M. L. et al.) 273–313 (Cambridge Univ. Press, 2007).
8. Vano, J. A. et al. Climate change impacts on water management and irrigated agriculture in the Yakima River Basin, Washington, USA. *Clim. Change* **102**, 287–317 (2010).
9. Vicuña, S., McPhee, J. & Garreaud, R. D. Agriculture vulnerability to climate change in a snowmelt-driven basin in semiarid Chile. *J. Water Resour. Plan. Manag.* **138**, 431–441 (2012).
10. Viviroli, D., Kummu, M., Meybeck, M., Kallio, M. & Wada, Y. Increasing dependence of lowland populations on mountain water resources. *Nat. Sustain.* **3**, 917 (2020).
11. Caretta, M. A. et al. in *Climate Change 2022: Impacts, Adaptation, and Vulnerability* (eds Pörtner, H.-O. et al.) 551–712 (Cambridge Univ. Press, 2022).
12. Lutz, A. F., Immerzeel, W. W., Shrestha, A. B. & Bierkens, M. F. P. Consistent increase in High Asia's runoff due to increasing glacier melt and precipitation. *Nat. Clim. Change* **4**, 587–592 (2014).
13. Biemans, H. et al. Importance of snow and glacier meltwater for agriculture on the Indo-Gangetic Plain. *Nat. Sustain.* **2**, 594–601 (2019).
14. Mankin, J. S., Viviroli, D., Singh, D., Hoekstra, A. Y. & Diffenbaugh, N. S. The potential for snow to supply human water demand in the present and future. *Environ. Res. Lett.* **10**, 114016 (2015).
15. Immerzeel, W. W. et al. Importance and vulnerability of the world's water towers. *Nature* **577**, 364–369 (2020).
16. Qin, Y. et al. Agricultural risks from changing snowmelt. *Nat. Clim. Change* **10**, 459–465 (2020).
17. Mekonnen, M. M. & Hoekstra, A. Y. A global and high-resolution assessment of the green, blue and grey water footprint of wheat. *Hydrol. Earth Syst. Sci.* **14**, 1259–1276 (2010).
18. Chapagain, A. K., Hoekstra, A. Y. & Savenije, H. H. G. Water saving through international trade of agricultural products. *Hydrol. Earth Syst. Sci.* **10**, 455–468 (2006).
19. Liu, W. F. et al. Savings and losses of global water resources in food-related virtual water trade. *WIREs Water* **6**, e1320 (2019).
20. Hoekstra, A. Y. & Hung, P. Q. Globalisation of water resources: international virtual water flows in relation to crop trade. *Glob. Environ. Change* **15**, 45–56 (2005).
21. Konar, M., Dalin, C., Hanasaki, N., Rinaldo, A. & Rodriguez-Iturbe, I. Temporal dynamics of blue and green virtual water trade networks. *Water Resour. Res.* **48**, W07509 (2012).
22. Dalin, C., Wada, Y., Kastner, T. & Puma, M. J. Groundwater depletion embedded in international food trade. *Nature* **553**, 366–366 (2018).
23. Liu, X. et al. Can virtual water trade save water resources? *Water Res.* **163**, 114848 (2019).
24. Pfister, S., Bayer, P., Koehler, A. & Hellweg, S. Environmental impacts of water use in global crop production: hotspots and trade-offs with land use. *Environ. Sci. Technol.* **45**, 5761–5768 (2011).
25. Lenzen, M. et al. International trade of scarce water. *Ecol. Econ.* **94**, 78–85 (2013).
26. O'Bannon, C., Carr, J., Seekell, D. A. & D'Odorico, P. Globalization of agricultural pollution due to international trade. *Hydrol. Earth Syst. Sci.* **18**, 503–510 (2014).
27. Mekonnen, M. M. & Hoekstra, A. Y. The green, blue and grey water footprint of crops and derived crop products. *Hydrol. Earth Syst. Sci.* **15**, 1577–1600 (2011).
28. Rosa, L., Chiarelli, D. D., Tu, C. Y., Rulli, M. C. & D'Odorico, P. Global unsustainable virtual water flows in agricultural trade. *Environ. Res. Lett.* **14**, 114001 (2019).
29. Liu, J. G., Yang, W. & Li, S. X. Framing ecosystem services in the telecoupled Anthropocene. *Front. Ecol. Environ.* **14**, 27–36 (2016).
30. Döll, P. & Siebert, S. Global modeling of irrigation water requirements. *Water Resour. Res.* **38**, 8-1–8-10 (2002).
31. Siebert, S. et al. Groundwater use for irrigation—a global inventory. *Hydrol. Earth Syst. Sci.* **14**, 1863–1880 (2010).
32. Qin, Y. et al. Flexibility and intensity of global water use. *Nat. Sustain.* **2**, 515–523 (2019).
33. Abatzoglou, J. T., Dobrowski, S. Z., Parks, S. A. & Hegewisch, K. C. Terraclimate, a high-resolution global dataset of monthly climate and climatic water balance from 1958–2015. *Sci. Data* **5**, 170191 (2018).
34. Peters, G. P., Andrew, R. & Lennox, J. Constructing an environmentally-extended multi-regional input-output table using the GTAP database. *Econ. Syst. Res.* **23**, 131–152 (2011).
35. Andrew, R. M. & Peters, G. P. A. A multi-region input–output table based on the Global Trade Analysis Project Database (GTAP-MRIO). *Econ. Syst. Res.* **25**, 99–121 (2013).
36. Jägermeyr, J. et al. Integrated crop water management might sustainably halve the global food gap. *Environ. Res. Lett.* **11**, 025002 (2016).
37. Brauman, K. A., Siebert, S. & Foley, J. A. Improvements in crop water productivity increase water sustainability and food security—a global analysis. *Environ. Res. Lett.* **8**, 024030 (2013).
38. MacDonald, G. K., D'Odorico, P. & Seekell, D. A. Pathways to sustainable intensification through crop water management. *Environ. Res. Lett.* **11**, 091001 (2016).
39. McDonald, R. I. et al. Water on an urban planet: urbanization and the reach of urban water infrastructure. *Glob. Environ. Change* **27**, 96–105 (2014).
40. Zhao, X. et al. Physical and virtual water transfers for regional water stress alleviation in China. *Proc. Natl Acad. Sci. USA* **112**, 1031–1035 (2015).
41. Kahil, M. T., Dinar, A. & Albiac, J. Modeling water scarcity and droughts for policy adaptation to climate change in arid and semiarid regions. *J. Hydrol.* **522**, 95–109 (2015).
42. Pritchard, H. D. Asia's shrinking glaciers protect large populations from drought stress. *Nature* **569**, 649–654 (2019).
43. Barnett, T. P., Adam, J. C. & Lettenmaier, D. P. Potential impacts of a warming climate on water availability in snow-dominated regions. *Nature* **438**, 303–309 (2005).
44. Immerzeel, W. W., van Beek, L. P. H. & Bierkens, M. F. P. Climate change will affect the Asian water towers. *Science* **328**, 1382–1385 (2010).
45. Bliss, A., Hock, R. & Radić, V. Global response of glacier runoff to twenty-first century climate change. *J. Geophys. Res. Earth* **119**, 717–730 (2014).
46. Huss, M. & Hock, R. Global-scale hydrological response to future glacier mass loss. *Nat. Clim. Change* **8**, 135–140 (2018).
47. Swann, A. L. S. Plants and drought in a changing climate. *Curr. Clim. Change Rep.* **4**, 192–201 (2018).

48. Wada, Y. et al. Modeling global water use for the 21st century: the Water Futures and Solutions (WFaS) initiative and its approaches. *Geosci. Model Dev.* **9**, 175–222 (2016).
49. *Sustainable Development Goals—Food Security and the Right to Food* (FAO, 2015); https://www.fao.org/sustainable-development-goals/background/fao-and-the-post-2015-development-agenda/food-security-and-the-right-to-food/en/
50. *The State of Food Security and Nutrition in the World* (FAO, 2020); http://www.fao.org/publications/sofi/2020/en/
51. *World Countries 2008 [Shapefile]* (ESRI, 2008); https://maps.princeton.edu/catalog/princeton-3r074w418

Methods

Subannual surface runoff and water demand

We obtain historical average monthly snowmelt runoff and rainfall runoff from the TerraClimate global climate and water balance dataset (1/24° × 1/24°) integrated with a water balance model for the period 1985–2015. The current version of TerraClimate's water balance model follows water balance procedures as described in ref. [52]. In doing so, monthly rainfall and snowmelt in excess of monthly evapotranspiration and soil moisture recharge are considered as surpluses. We also conduct sensitivity studies in separating surface and baseflow[53] in simulating snowmelt and rainfall runoff (Supplementary Fig. 20). Earlier studies have extensively evaluated TerraClimate, demonstrating strong validation in comparison to observations[16,33]. More details of this dataset are described in ref. [33]. Here, we provide a series of additional TerraClimate subannual runoff, snow water equivalent and snow fraction validations, which demonstrate reasonable global performance (Supplementary Notes, Supplementary Figs. 21–24 and Supplementary Tables 1 and 2). Similar to other global products, TerraClimate acknowledges challenges in resolving precipitation in mountainous regions[54], although it does not have any systematic over- or under-estimation. Historical grid-level snowmelt runoff and rainfall runoff are then aggregated for global basins as used in earlier global studies[14,16,55,56] without accounting for routing, this can be a potential limitation for large-size basins, such as Nile, Mississippi and Niger[57].

We further simulate snowmelt and rainfall runoff under two global climate warming scenarios (2 °C and 4 °C above pre-industrial global mean temperature), using the pattern scaling approach to superpose changes in 1985–2015 TerraClimate monthly climate variables (for example, temperature and precipitation) together with the water balance model. Details of the pattern scaling approach are described in ref. [16]. Essentially, we acquire multimodel median scaling factors for monthly climate variables based on climate projections from 23 Coupled Model Intercomparison Project Phase 5 climate models for two 30-yr periods: pre-industrial period (1850–1879) using the historical forcing and end-of-century period (2070–2099) with the representative concentration pathway RCP 8.5 forcing. We thus develop future climate scenarios via incorporating the historical TerraClimate data (1985–2015) with the multimodel scaling factors. As emphasized in ref. [16], computationally inexpensive pattern scaling approach has the advantage of being downscaled to global high spatial resolution (1/24° × 1/24°) and allows the flexibility for interoperability between uncertainty inherent in different emission scenarios, time periods and model choices, and can be more directly linked to policy-relevant goals such as 2 °C and 4 °C warming scenarios above pre-industrial levels. Notably, the scaling approach does retain changes in interannual and seasonal variability in climate change scenarios, which are advantageous properties for the analysis in this study. Although we use multimodel median scaling factors to provide a central estimate of future changes, Supplementary Fig. 25 illustrates model spreads in scaling factors for land warming and precipitation. We acknowledge potential uncertainties resulting from the spread of different climate models and follow-up work to further decompose uncertainty chains are needed. Notably, the pattern scaling approach is only used to obtain the 2 °C and 4 °C monthly climate variables (for example, temperature and precipitation), on the basis of which we further run the water balance model to simulate snowmelt and rainfall runoff.

Monthly irrigation water consumption (1/12° × 1/12°) for 26 crop species during the same period of 1985–2015 are calculated with the GCWM based on daily soil water balances[58]. GCWM estimates irrigation water use on the basis of the Penman–Monteith equation, which integrates crop-specific monthly growing areas, cropping calendars, together with climate input variables (wind speed, temperature and precipitation) at daily time steps[59–61]. Details of GCWM are described in a series of earlier studies[58,62]. Although GCWM factors in both intra-annual and interannual climate variability, it keeps land area constant at the MIRCA2000 (monthly irrigated and rainfed crop areas around the year 2000, 1998–2002) level due to lack of alternative time series data for irrigated and rainfed crop areas. To factor in impacts of both climate variability and land area changes on irrigation water demand, following earlier estimates[16,32], we adjust the GCWM-simulated irrigation water consumption using the FAOSTAT database, which provides yearly country-level data for area equipped with irrigation[63]. Specifically, we first estimate the ratio of area equipped with irrigation in the actual year to area equipped for irrigation according to the MIRCA2000 reference year (1998–2002 average) for each country using the FAO data. Then we use this ratio to scale GCWM-simulated yearly irrigation water consumption for each grid belonging to each country[16,32] (equation (1)). Additionally, we quantify monthly crop-specific surface irrigation water consumption on the basis of grid-level share of surface water to groundwater for irrigation purposes[32]. Monthly non-irrigation water demand is extracted from earlier studies at the same spatial resolution to provide representative historical industrial and domestic water demand[64]. We apply the same grid-level surface-water fraction for the agriculture sector to water uses in non-agriculture sectors following an earlier study[16].

$$\mathrm{Irr}_{i,c,s} = \frac{\mathrm{AEI}_{i,c}}{\mathrm{AEI}_{\mathrm{ref},c}} \times \mathrm{Irr}_{\mathrm{GCWM},i,c,s} \quad (1)$$

Where $\mathrm{Irr}_{i,c,s}$ refers to irrigation water consumption for year i, country c and crop species s; $\mathrm{Irr}_{\mathrm{GCWM}}$ refers to GCWM-simulated irrigation water consumption; and $\mathrm{AEI}_{i,c}$ and $\mathrm{AEI}_{\mathrm{ref},c}$ refer to country-level (c) area equipped with irrigation (AEI) for year i and the reference year (1998–2002 average) from the FAOSTAT dataset, respectively.

GTAP region-level agricultural snowmelt consumption

As illustrated in Supplementary Fig. 26, aggregating grid-level historical runoff (1/24° × 1/24°) from TerraClimate (green grids) and historical water demand (1/12° × 1/12°) mainly from the GCWM (black grids) to the same global major river basins (a modified version of the Simulated Topological Network 30p)[14] (for example, basin A), we compare basin-level monthly historical runoff (snowmelt and rainfall runoff) and monthly total surface-water demand. In this way, we quantify crop-specific snowmelt runoff consumption, rainfall runoff consumption and alternative water demand (cross-region transfers and reservoir storage) in each month for each basin. When basin-level runoff is above total surface-water demand, we calculate monthly total snowmelt runoff consumption on the basis of basin total surface-water demand and the share of runoff coming from snowmelt. The underlying assumption is that snowmelt runoff and rainfall runoff have the same priority in meeting irrigation water demand[16] and no alternative water demand is needed in this case. However, if monthly basin total surface-water demand surpasses total surface runoff, all available monthly snowmelt and rainfall runoff within the basin will be consumed. Meanwhile, the insufficiency is met by alternative surface supplies that can come from water storage, cross-region transfer, more groundwater pumping and desalination, assuming historical water demand is fully met, although alternative water supply may have been attained at high costs[16]. We then quantify monthly crop-specific irrigation snowmelt runoff consumption by monthly total snowmelt runoff consumption and the share of corresponding irrigation surface-water demand to total surface-water demand, assuming water demands from different sectors have the same water allocation priority. Lacking global-scale irrigation supply infrastructure information to track the routing of water for irrigation, we assume snowmelt and rainfall runoff can generally be used within the basin via irrigation supply canals and acknowledge that this may cause potential uncertainties. Sensitivity studies are conducted to evaluate the potential impacts due to different cross-sector water allocation strategies and groundwater fractions (Supplementary Notes and Supplementary Fig. 27). As integrated models that can simultaneously provide high spatial–temporal resolution snowmelt runoff and irrigation water

demand data are relatively underdeveloped, we bring the TerraClimate and GCWM models together. Although these are developed separately, the resulting uncertainties are likely to be small as main variables impacting irrigation water requirement are long-term (for example, weeks or months) precipitation (in subhumid regions) or temperature (in arid regions), which generally have good agreement across different historical climate input data. Additionally, both TerraClimate and GCWM use Climatic Research Unit datasets as a key historical climate input data that could further alleviate the resulting inconsistences.

Integrating basin-level, source-specific water consumption estimated above with the spatial distribution of crop-specific surface irrigation water demand within each basin provided by GCWM, we estimate grid-level crop-specific snowmelt runoff, rainfall runoff and alternative water consumption at the same spatial resolution as crop-specific irrigation water demand (Supplementary Fig. 26). Aggregating grids belonging to each of the GTAP regions, we thus obtain the consumption of snowmelt runoff, rainfall runoff and alternative water at the 141 GTAP region level as defined by GTAP v.10 (refs. [34,35]; https://www.gtap.agecon.purdue.edu/databases/regions.aspx?version=10.211). For basins that are completely within the targeted GTAP region (Supplementary Fig. 26a), all grids within the basin are also within the GTAP region; yet for transboundary basins, we only aggregate source- and crop-specific water consumption for grids that are simultaneously within the basin and the targeted GTAP region (for example, R), while allocating water consumption in basin A in remaining grids to their respective GTAP regions (for example, R2; Supplementary Fig. 26b). Such aggregation will potentially cause uncertainties especially for transboundary basins and as earlier studies[65], we caution the interpretation of results moving along spatial scales. Nevertheless, this is based on the best-available data given it is global in nature and differences in the spatial resolution between water management and trade flow; and we do acknowledge that follow-up local/regional studies cannot be substituted for but potentially be guided through the integrated framework built in our global analysis. We then quantify the 31-yr average (1985–2015) monthly and annual average regional total water consumption from three sources under both the baseline and the 2 °C and 4 °C warming scenarios (Fig. 1).

In each GTAP region, we calculate snowmelt consumption ratio as the share of regional total irrigation surface-water demand met by snowmelt runoff, which indicates the snowmelt availability during crop growing seasons. We then characterize snowmelt-dependent GTAP regions on the basis of earlier snowmelt dependence definitions[16]: GTAP regions require notable amounts of surface water for irrigation (≥1 mm yr^{-1}) and a relatively large portion of surface irrigation water (≥5%) is contributed by snowmelt runoff. We thus identify production-based snowmelt dependence for global GTAP regions on the basis of where irrigated agriculture is produced (attributing water consumption to where agricultural production occurs) (Fig. 3). Notably, as we characterize snowmelt dependence on the basis of the above two-dimensional standards, thresholds are chosen to identify global hotspots where irrigated agriculture is relatively more dependent on snowmelt runoff in comparison to other regions. Here, we keep cross-sector water demand under warming scenarios the same as that during the historical periods across sectors due to large uncertainties in accurately quantifying future global water demand at high spatial–temporal resolutions. For instance, counteracting mechanisms affect irrigation water consumption in opposing directions with increasing CO_2 (for example, increasing evapotranspiration yet higher water use efficiency)[47], while location-specific information such as land use changes, growing seasons changes and farmers' adaptation strategies (for example, crop switching) are not easily available across the globe[48]. Nevertheless, we conduct sensitivity analyses to evaluate the impacts of changing water demand on our characterized snowmelt dependence (Supplementary Fig. 14). Similarly, we evaluate the impacts of varying cross-sector water allocation priority setting and changing the relative fraction of groundwater consumption on the characterization of global snowmelt dependence (Supplementary Fig. 27). In the GTAP v.10 regional classification, Yemen is grouped into 'Rest of Western Asia' together with Iran, which have noticeable differences in snowmelt availability. To avoid confusion in interpretation, we separate Yemen from the other Rest of Western Asia regions for presentation purposes in our maps, assuming that the share of snowmelt consumption in the Rest of Western Asia total for Yemen is the same before and after trade.

Irrigated agriculture is exposed to changing snowmelt risks due to both decreasing magnitude of snowmelt runoff and earlier snow melting[5,7,9]. Repeating the above comparisons for the 2 °C and 4 °C warming scenarios, we hence obtain basin-level water consumption from three sources under the warming climate. We then identify basins exposed to snowmelt risks as those snow-dependent ones which are simultaneously subjected to decreases in snowmelt consumption ratio (share of surface irrigation demand met by snowmelt runoff) and increases in alternative water demand ratio (share of irrigation surface-water demand met by alternative water supply) under the 2 °C and 4 °C warming scenario, respectively (Supplementary Fig. 10), as defined in an earlier study[16]. Alternative water sources can come from interbasin water transfer, more groundwater pumping or expanding reservoir storage; however, such strategies may have unintended side effects resulting from expanding water storage and reservoir reliance[66,67], as well as unsustainable groundwater use[68].

Agricultural production exposed to snowmelt risks

The Food and Agriculture Organization of the United Nations database (FAO)[63] provides the 'best-available' crop-specific (s) country (c) total food production (TOT), although with no information about the relative share of irrigated (IRR) and rainfed (RFD) production and their respective spatial distribution within the country. Combined with statistics of entity-level crop yields (country, federal state, province and so on), GCWM simulates grid-level crop-specific irrigated and rainfed agriculture production for 26 crop species at the spatial resolution of 1/12° × 1/12° (ref. [58]). Methodology details are summarized in ref. [58]. Therefore, by scaling GCWM-simulated grid-level (i) irrigated and rainfed production in each country on the basis of FAO statistic data for country total production ($\mathrm{FAO_{TOT}}, c$) and applying grid-level fraction of groundwater use (GF)[31], we obtain grid-level surface-water-irrigated agricultural production ($\mathrm{GCWM_{IRR}} - \mathrm{adj} - \mathrm{surf}, c, i$) that makes the best use of available datasets and modelling tools (equations (2)–(7)). Coupling our estimates of surface-water-irrigated agriculture production with identified basins at risk under climate change, we quantify the surface-water-irrigated agricultural production exposed to snowmelt risks (that is, production at risk) under the 2 °C and 4 °C warming scenarios, respectively (Extended Data Figs. 3 and 4).

$$\mathrm{GCWM_{TOT}}, s, c = \sum_{i=1}^{n} (\mathrm{GCWM_{RFD}}, s, c, i + \mathrm{GCWM_{IRR}}, s, c, i) \quad (2)$$

$$\mathrm{SF_{TOT}}, s, c = \mathrm{FAO_{TOT}}, s, c / \mathrm{GCWM_{TOT}}, s, c \quad (3)$$

$$\mathrm{GCWM_{RFD}} - \mathrm{adj}, s, c, i = \mathrm{GCWM_{RFD}}, s, c, i \times \mathrm{SF_{TOT}}, s, c \quad (4)$$

$$\mathrm{GCWM_{IRR}} - \mathrm{adj}, s, c, i = \mathrm{GCWM_{IRR}}, s, c, i \times \mathrm{SF_{TOT}}, s, c \quad (5)$$

$$\mathrm{GCWM_{IRR}} - \mathrm{adj} - \mathrm{ground}, s, c, i = \mathrm{GCWM_{IRR}} - \mathrm{adj}, s, c, i \times \mathrm{GF}_i \quad (6)$$

$$\mathrm{GCWM_{IRR}} - \mathrm{adj} - \mathrm{surf}, s, c, i = \mathrm{GCWM_{IRR}} - \mathrm{adj}, s, c, i \times (1 - \mathrm{GF}_i) \quad (7)$$

Here, $\mathrm{GCWM_{RFD}}, s, c, i$, $\mathrm{GCWM_{IRR}}, s, c, i$ and $\mathrm{GCWM_{TOT}}, s, c$ refer to GCWM-simulated rainfed production (RFD), irrigated production (IRR) and the sum of rainfed and irrigated production (TOT) for crop s in

country c and grid i. SF_{TOT}, s, c refers to country-level scaling factors between FAO statistics and GCWM-simulated country total production for crop s in country c. Then we use the scaling factors to estimate grid-level FAO-adjusted rainfed $(GCWM_{RFD} - adj, s, c, i)$ and irrigated $(GCWM_{IRR} - adj, s, c, i)$ production. GF_i represents the relative fraction of groundwater used for irrigation to total irrigation water in grid i, on the basis of which we estimate the fraction of grid-level surface-water-irrigated production.

Virtual transfer of snowmelt runoff and production at risk

We use a global MRIO model based on the GTAP v.10 database to obtain its latest publicly available multiregion flow matrix for agricultural products in 2014. GCWM simulates irrigation water consumption for global crops categorized into 26 crop species. In addition to simulating water consumption for 24 individual major crop species, including wheat, rice, maize, barley, rye, millet, sorghum, soybeans, sunflower, potatoes, cassava, sugar cane, sugar beets, rapeseed/canola, groundnuts/peanuts, pulses, grapes/vine, cotton, managed grassland/pasture, citrus, date palm, coffee, cocoa and oil palm, it also simulates over one-hundred subcrop species as two aggregated categories: 'other annuals' and 'other perennials'. We assume no international trade for grassland according to the GTAP v.10 database. Following earlier studies[69,70], we thus map all crop species to the corresponding eight GTAP agricultural products, including wheat, paddy rice, oil seeds, vegetables/fruits/nuts, sugar cane/beet, plant fibres, other cereal grains and other crops. For other perennials and other annuals, which together account for ~13% of total surface irrigation water consumption, we assume their respective subcategory water consumption is proportional to their calorie production without better information[32]. Sensitivity studies are conducted to evaluate the associated uncertainty (Supplementary Fig. 28). Aggregating crop-specific grid-level water consumption (total surface water, snowmelt runoff, rainfall runoff and alternative water) to their corresponding GTAP categories, we quantify irrigation water transfer embodied in international trade on the basis of the MRIO model. The MRIO model, which is capable of tracking the whole supply chain to differentiate between intermediate and final consumers (hence tracking 're-exports'), has been widely used in previous studies[25,71–75]. In the MRIO framework, the monetary balance can be represented as

$$\begin{bmatrix} x^1 \\ x^2 \\ \vdots \\ x^r \\ \vdots \\ x^n \end{bmatrix} = \begin{bmatrix} A^{11} & A^{12} & \cdots & A^{1r} & \cdots & A^{1n} \\ A^{21} & A^{22} & \cdots & A^{2r} & \cdots & A^{2n} \\ \vdots & \vdots & \ddots & \vdots & \vdots & \vdots \\ A^{r1} & A^{r2} & \cdots & A^{rr} & \cdots & A^{rn} \\ \vdots & \vdots & \vdots & \vdots & \ddots & \vdots \\ A^{n1} & A^{n2} & \cdots & A^{nr} & \cdots & A^{nn} \end{bmatrix} \begin{bmatrix} x^1 \\ x^2 \\ \vdots \\ x^r \\ \vdots \\ x^n \end{bmatrix} + \begin{bmatrix} \Sigma_s y^{1s} \\ \Sigma_s y^{2s} \\ \vdots \\ \Sigma_s y^{rs} \\ \vdots \\ \Sigma_s y^{ns} \end{bmatrix} \quad (8)$$

where x^r is a vector of sectoral specific total outputs in region r; y^{rs} is a vector of the finished products consumed in region s but produced in region r and A^{rs} is a normalized matrix of intermediate consumption coefficients. In matrix form, equation (1) can be simplified as: $x = Ax + y$.

By solving the equation, we can yield the following equation:

$$x = (I - A)^{-1} y \quad (9)$$

where $(I - A)^{-1}$ is the Leontief inverse matrix and I is the identity matrix.

Under this MRIO framework, we can calculate region- and sector-specific production related to the final consumption activity of a given region on the basis of the following equation:

$$x^s_{com} = (I - A)^{-1} y^s_{com} \quad (10)$$

where $y^s_{com} = (y^{1s} \ldots y^{rs} \ldots y^{ns})'$ is a vector of sector-specific final consumption in region s, $x^s_{com} = (x^{1s} \ldots x^{rs} \ldots x^{ns})'$ is a vector of sector-specific production by region associated with final consumption in region s. Thus, the fraction of region- and sector-specific production related to consumption in region s (f^s_{com}) can be calculated as:

$$f^s_{com} = x^s_{com} ./ x \quad (11)$$

Using the above MRIO model, we re-attribute the production of different agricultural products throughout the global supply chains to regions where related goods are ultimately consumed. By further combining sector-specific water consumption, we can estimate the virtual transfer of agricultural water consumption, crop-specific surface-water-fed production and production exposed to snowmelt risks for each GTAP region. Without better information, trade flows are considered similar for crops irrigated with groundwater or with surface water.

Accounting for irrigation snowmelt runoff, rainfall runoff, alternative water flow embodied in trade, together with total surface-water-irrigated agricultural production and production at risk, we quantify their respective consumption-based accounting in each GTAP region, as well as the resulting telecouplings in snowmelt dependence and snowmelt risks. For instance, we define consumption-based GTAP-level snowmelt dependence on the basis of GTAP-level regional average irrigation surface-water consumption and the relative share of that water contributed by snowmelt runoff, both of which are calculated on the basis of where final products are consumed (attributing water consumption to where final products consumption occurs).

Here, we use the MRIO model supported by the GTAP dataset, which distinguishes intermediate and final products and thus track the virtual water flow across the whole supply chain. In addition, a physical trade flow (PTF) model based on FAOSTAT bilateral trade data, which suffers from the truncation error yet has much more detailed crop categories[76], is also used to estimate the virtual flow to provide a complementary perspective[77] (Supplementary Notes). Notably, the MRIO and PTF models are different regarding aims, system boundaries and trading metrics[77]. The MRIO model tracks indirect monetary trade flows all the way to final consumption, yet the FAO trade data tracks physical products up to where they are physically consumed[77,78]. Therefore, MRIO analysis is more suitable for consumption-based accounting which follows the virtual water flow through the whole supply chain to where final consumption takes place[77,78]. Despite differences in the virtual flow of source-specific surface irrigation water consumption (for example, snowmelt runoff and rainfall runoff), both GTAP and FAOSTAT-based results demonstrate evident snowmelt dependence and risk diffusion (Fig. 3 and Supplementary Figs. 13 and 16–18) and consistent snowmelt risks importing in western Europe and other countries (Supplementary Figs. 13 and 18).

Data availability

GTAP is available from: https://www.gtap.agecon.purdue.edu/. GCWM outputs are available from: https://www.uni-frankfurt.de/45217988/Global_Crop_Water_Model_GCWM. TerraClimate data are available from: http://www.climatologylab.org/terraclimate.html. FAO data are available from: https://www.fao.org/faostat/en/#data. All other data that support the findings of this study are available in the main text or the supplementary materials. Source data are provided with this paper.

Code availability

Computer code or algorithm used to generate results that are reported in the paper and central to the main claims are available from figshare[79].

References

52. Dobrowski, S. Z. et al. The climate velocity of the contiguous United States during the 20th century. *Glob. Change Biol.* **19**, 241–251 (2013).
53. Miller, O. L. et al. How will baseflow respond to climate change in the upper colorado river basin? *Geophys. Res. Lett.* **48**, e2021GL095085 (2021).

54. Lundquist, J., Hughes, M., Gutmann, E. & Kapnick, S. Our skill in modeling mountain rain and snow is bypassing the skill of our observational networks. *Bull. Am. Meteorol. Soc.* **100**, 2473–2490 (2019).
55. Vörösmarty, C. J., Fekete, B. M., Meybeck, M. & Lammers, R. B. Geomorphometric attributes of the global system of rivers at 30-minute spatial resolution. *J. Hydrol.* **237**, 17–39 (2000).
56. Meybeck, M., Dürr, H. H. & Vörösmarty, C. J. Global coastal segmentation and its river catchment contributors: a new look at land–ocean linkage. *Glob. Biogeochem. Cycles* **20**, GB1S90 (2006).
57. Allen, G. H., David, C. H., Andreadis, K. M., Hossain, F. & Famiglietti, J. S. Global estimates of river flow wave travel times and implications for low-latency satellite data. *Geophys. Res. Lett.* **45**, 7551–7560 (2018).
58. Siebert, S. & Döll, P. Quantifying blue and green virtual water contents in global crop production as well as potential production losses without irrigation. *J. Hydrol.* **384**, 198–217 (2010).
59. Siebert, S. et al. Development and validation of the global map of irrigation areas. *Hydrol. Earth Syst. Sci.* **9**, 535–547 (2005).
60. Siebert, S., Henrich, V., Frenken, K. & Burke, J. *Update of the Digital Global Map of Irrigation Areas to Version 5* (FAO, 2013); https://www.fao.org/3/I9261EN/i9261en.pdf
61. Siebert, S., Döll, P., Feick, S., Hoogeveen, J. & Frenken, K. *Global Map of Irrigation Areas Version 4.0.1 [CD-ROM]* (FAO, 2007).
62. Siebert, S. & Döll, P. *The Global Crop Water Model (GCWM): Documentation and First Results for Irrigated Crops* (Institute of Physical Geography, 2008).
63. *Food and Agriculture Data* (FAO, 2018); http://www.fao.org/faostat/en/#data
64. Hoekstra, A. Y., Mekonnen, M. M., Chapagain, A. K., Mathews, R. E. & Richter, B. D. Global monthly water scarcity: blue water footprints versus blue water availability. *PLoS ONE* **7**, e32688 (2012).
65. Greve, P. et al. Global assessment of water challenges under uncertainty in water scarcity projections. *Nat. Sustain.* **1**, 486–494 (2018).
66. Rosa, L. et al. Potential for sustainable irrigation expansion in a 3 °C warmer climate. *Proc. Natl Acad. Sci. USA* **117**, 29526–29534 (2020).
67. Baldassarre, G. D. et al. Water shortages worsened by reservoir effects. *Nat. Sustain.* **1**, 617–622 (2018).
68. Sneed, M., Brandt, J. T. & Solt, M. *Land Subsidence along the Delta-Mendota Canal in the Northern Part of the San Joaquin Valley, California, 2003–2010* (USGS, 2013); http://pubs.usgs.gov/sir/2013/5142/
69. Hong, C. P. et al. Global and regional drivers of land-use emissions in 1961–2017. *Nature* **589**, 554 (2021).
70. *Technical Conversion Factors for Agricultural Commodities* (FAO, 2015); http://www.fao.org/fileadmintemplates/ess/documents/methodology/tcf.pdf
71. Feng, K. S. & Hubacek, K. in *Handbook of Research Methods and Applications in Environmental Studies* (ed. Ruth, M.) Ch. 10 (Edward Elgar Publishing, 2015).
72. Feng, K. S., Chapagain, A., Shu, S., Pfister, S. & Hubacek, K. Comparison of bottom-up and top-down approaches to calculating the water footprints of nations. *Econ. Syst. Res.* **23**, 371–385 (2011).
73. Chen, Z. M. & Chen, G. Q. Virtual water accounting for the globalized world economy: national water footprint and international virtual water trade. *Ecol. Indic.* **28**, 142–149 (2013).
74. Davis, S. J., Peters, G. P. & Caldeira, K. The supply chain of CO_2 emissions. *Proc. Natl Acad. Sci. USA* **108**, 18554–18559 (2011).
75. Davis, S. J. & Caldeira, K. Consumption-based accounting of CO_2 emissions. *Proc. Natl Acad. Sci. USA* **107**, 5687–5692 (2010).
76. Hubacek, K. & Feng, K. S. Comparing apples and oranges: some confusion about using and interpreting physical trade matrices versus multi-regional input-output analysis. *Land Use Policy* **50**, 194–201 (2016).
77. Pendrill, F. et al. Agricultural and forestry trade drives large share of tropical deforestation emissions. *Glob. Environ. Change* **56**, 1–10 (2019).
78. Henders, S., Persson, U. M. & Kastner, T. Trading forests: land-use change and carbon emissions embodied in production and exports of forest-risk commodities. *Environ. Res. Lett.* **10**, 125012 (2015).
79. Qin, Y. Snow trade 2022. figshare https://doi.org/10.6084/m9.figshare.21076117 (2022).

Acknowledgements

This work was supported by the National Natural Science Foundation of China grant no. 42277482 to Y.Q., the Foundation for Food and Agriculture Research through a New Innovator Award to N.D.M., the US National Science Foundation INFEWS grant EAR 1639318 to S.J.D., the German Federal Ministry of Education and Research (BMBF; grant no. 02WGR1642A) through its Global Resource Water (GRoW) funding initiative and the German Research Foundation SFB 1502/1-2022-Project no. 450058266 to S.S., the University of California, Division of Agriculture and Natural Resources California Institute for Water Resources and US Geological Survey grant G21AP10611-00 and a California State University Water Resources and Policy Initiatives grant to L.S.H., the Scientific Research Start-up Funds (QD2021030C) from Tsinghua Shenzhen International Graduate School to C.H., the USDA-NIFA award (2021-69012-35916) to J.T.A. and National Natural Science Foundation of China grant no. 71904097 to H.Z. We acknowledge helpful discussions with D. Li and P. Lin.

Author contributions

Y.Q., N.D.M. and S.J.D. designed the study. Y.Q. performed the analyses, with additional support from C.H., H.Z., S.S., J.T.A., L.S.H., L.L.S., S.P. and S.Y.L. on datasets and analytical approaches. Y.Q., N.D.M., S.J.D., S.S., T.Z. and D.M. led the writing with input from all coauthors.

Competing interests

The authors declare no competing interests.

Additional information

Extended data is available for this paper at https://doi.org/10.1038/s41558-022-01509-z.

Supplementary information The online version contains supplementary material available at https://doi.org/10.1038/s41558-022-01509-z.

Correspondence and requests for materials should be addressed to Yue Qin or Nathaniel D. Mueller.

Peer review information *Nature Climate Change* thanks Ian Holman, Wenfeng Liu, Landon Marston and the other, anonymous, reviewer(s) for their contribution to the peer review of this work.

https://doi.org/10.1038/s41558-022-01509-z

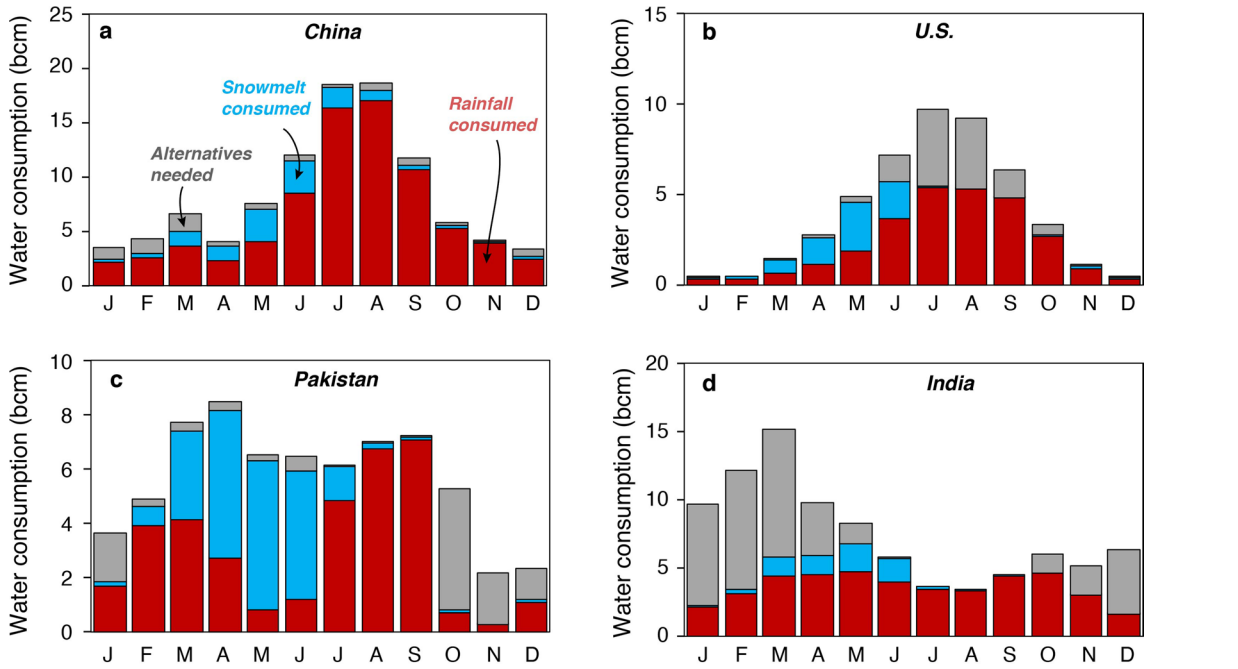

Extended Data Fig. 1 | Source-specific water demand for major countries under a 2 °C warming scenario. GTAP region-level surface-water demand met by different water sources under the +2 °C warming scenario. Monthly runoff from snowmelt runoff, rainfall runoff, and alternative water demand for **(a)** China, **(b)** U.S., **(c)** Pakistan, and **(d)** India are shown in stacked bars inside the box, where the shaded red, blue and grey bars denote the corresponding contributions from rainfall, snowmelt, and alternative surface-water sources (that is, reservoirs storage and interbasin transfer), respectively.

https://doi.org/10.1038/s41558-022-01509-z

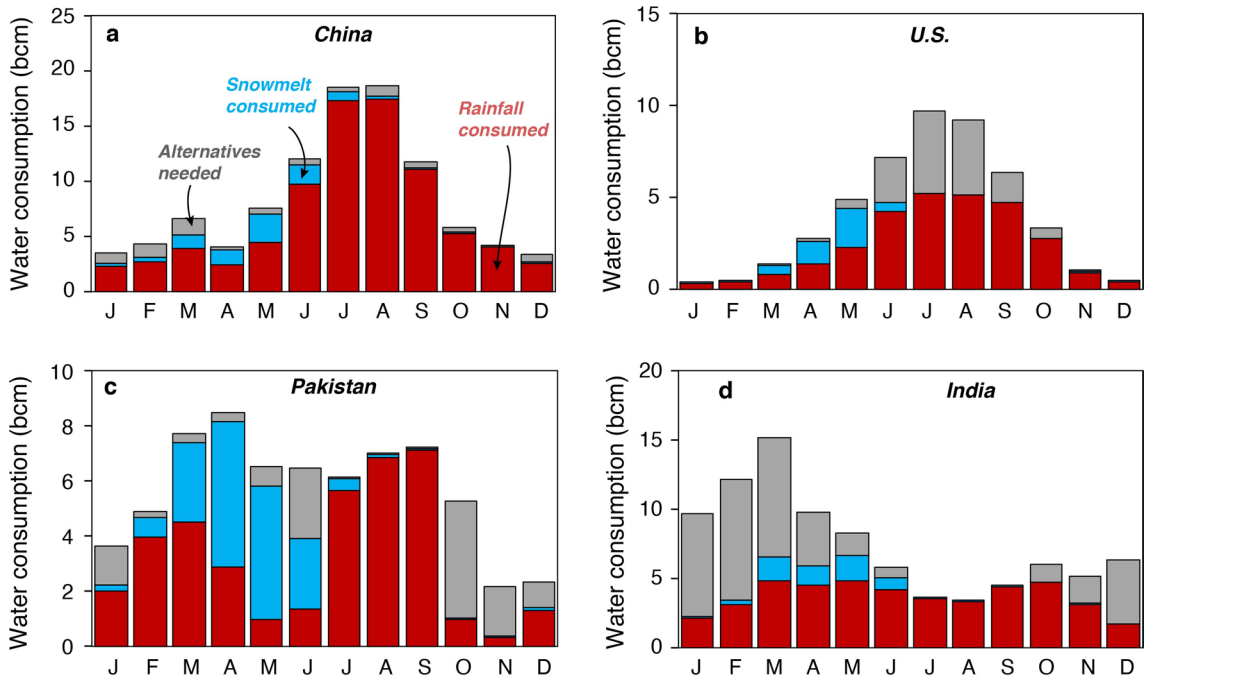

Extended Data Fig. 2 | Source-specific water demand for major countries under a 4 °C warming scenario. GTAP region-level surface-water demand met by different water sources under the +4 °C warming scenario. Monthly runoff from snowmelt runoff, rainfall runoff, and alternative water demand for **(a)** China, **(b)** U.S., **(c)** Pakistan, and **(d)** India are shown in stacked bars inside the box, where the shaded red, blue and grey bars denote the corresponding contributions from rainfall, snowmelt, and alternative surface-water sources (that is, reservoirs storage and interbasin transfer), respectively.

https://doi.org/10.1038/s41558-022-01509-z

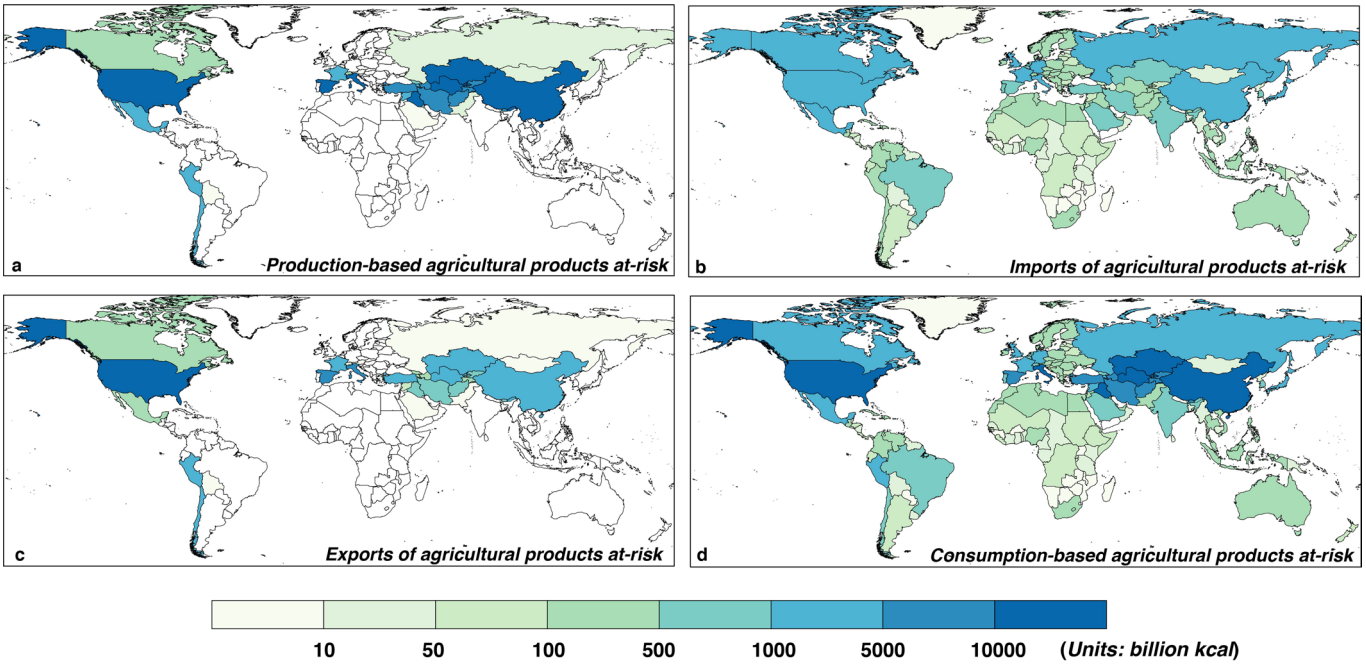

Extended Data Fig. 3 | Virtual transfer of agricultural production at risk under the 2 °C warming scenario. GTAP-level agricultural production at risk under the 2 °C warming scenario and virtual transfer throughout the whole global supply chains. GTAP-level **(a)** surface-water-irrigated agricultural products exposed to snowmelt risks under production-based accounting, **(b)** imports of surface-water-irrigated agricultural products at risk embodied in trade, **(c)** exports of surface-water-irrigated agricultural products at risk embodied in trade, and **(d)** surface-water-irrigated agricultural products exposed to snowmelt risks under consumption-based accounting.

https://doi.org/10.1038/s41558-022-01509-z

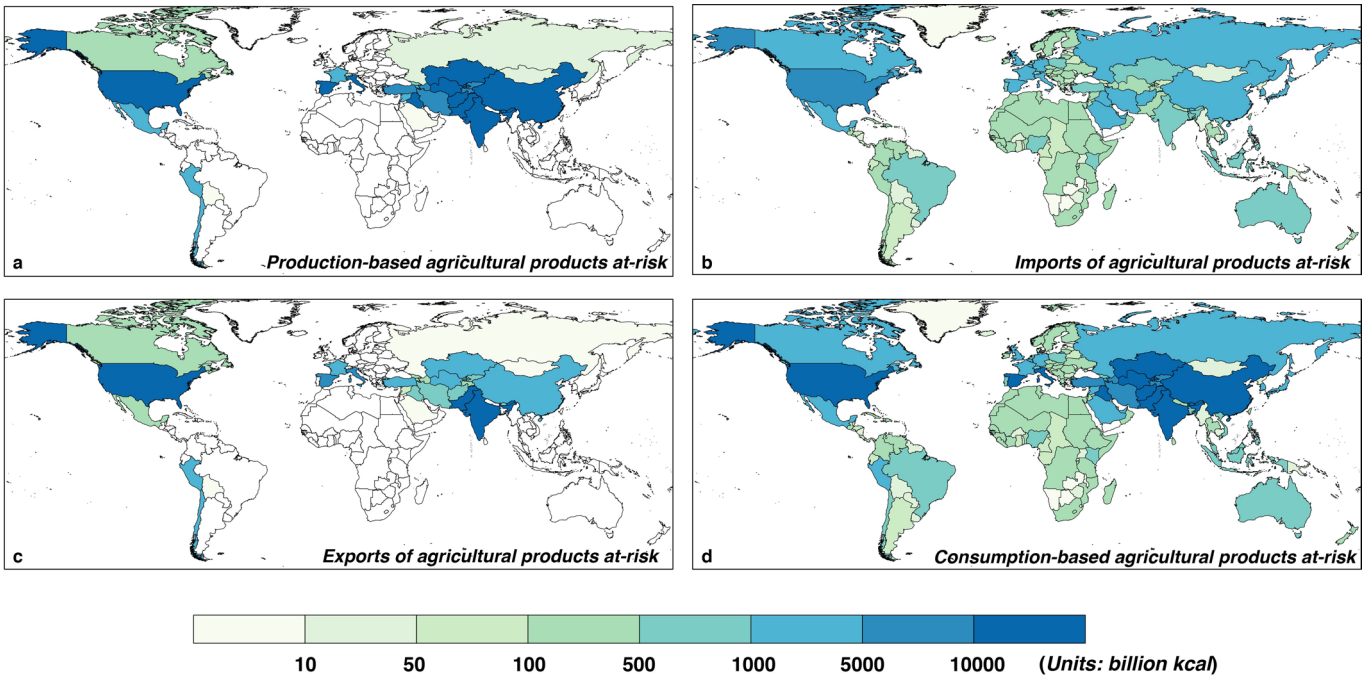

Extended Data Fig. 4 | Virtual transfer of agricultural production at risk under the 4 °C warming scenario. GTAP-level agricultural production at risk under the 4 °C warming scenario and virtual transfer throughout the whole global supply chains. GTAP-level **(a)** surface-water-irrigated agricultural products exposed to snowmelt risks under production-based accounting, **(b)** imports of surface-water-irrigated agricultural products at risk embodied in trade, **(c)** exports of surface-water-irrigated agricultural products at risk embodied in trade, and **(d)** surface-water-irrigated agricultural products exposed to snowmelt risks under consumption-based accounting.